

### Aromatic vs Aliphatic C–H Cleavage of Alkyl-Substituted Pyridines by (PNP<sup>iPr</sup>)Re Compounds

Oleg V. Ozerov,<sup>†</sup> Maren Pink, Lori A. Watson, and Kenneth G. Caulton\*

Contribution from the Department of Chemistry, Indiana University,  
Bloomington, Indiana 47405

Received July 1, 2003; E-mail: caulton@indiana.edu

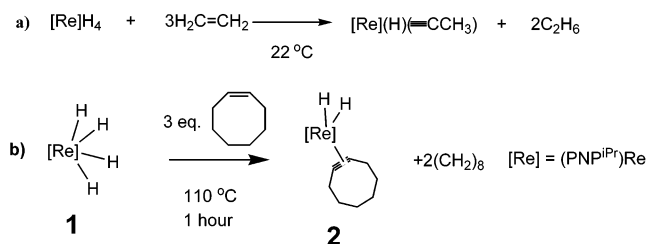
**Abstract:** Both (PNP)Re(H)<sub>4</sub> and (PNP)ReH(cyclooctyne) (PNP<sup>iPr</sup> = (iPr<sub>2</sub>PCH<sub>2</sub>SiMe<sub>2</sub>)<sub>2</sub>N) react with alkylpyridines NC<sub>5</sub>H<sub>4</sub>R to give first (PNP)ReH<sub>2</sub>(η<sup>2</sup>-pyridyl) and cyclooctene and then, when not sterically blocked, (PNP)Re(η<sup>2</sup>-pyridyl)<sub>2</sub> and cyclooctane. The latter are shown by NMR, X-ray diffraction, and DFT calculations to have several energetically competitive isomeric structures and pyridyl N donation in preference to PNP amide π-donation. DFT studies support NMR solution evidence that the most stable bis pyridyl structure is one that is doubly η<sup>2</sup>- with the pyridyl N donating to the metal center. When both ortho positions carry methyl substituents, cyclooctane and the carbyne complex (PNP)ReH(≡C-pyridyl) are produced. Excess 2-vinyl pyridine reacts with (PNP)Re(H)<sub>4</sub> preferentially at the vinyl group, to give 2-ethyl pyridine and the σ-vinyl complex (PNP)ReH[η<sup>2</sup>-CH=CH(2-py)]. The DFT and X-ray structures show, by various comparisons, the ability of the PNP amide nitrogen to π-donate to an otherwise unsaturated d<sup>4</sup> Re<sup>III</sup> center, showing short Re–N distances consistent with the presence of π-donation.

#### Introduction

The fragment (PNP)Re (Scheme 1) has the ability to transform ethylene<sup>1</sup> and other olefins<sup>2</sup> to hydrido carbynes (Scheme 1). Transformation of small molecules into ligands with a multiple metal–carbon bond must be viewed as characteristic of highly basic and reducing metal centers.<sup>3–10</sup> Re, devoid of any significant π-acid ligand, certainly falls into such a category.

We were interested in further evaluating the reactivity of this fragment, this time toward substituted pyridines. Pyridines and other heterocycles are especially interesting substrates for metal-catalyzed reactions. Pyridines are a ubiquitous presence in transition metal chemistry. The more classical mode of coordination of pyridines is η<sup>1</sup>-coordination via the lone pair of N, i.e., pyridine acts as a simple neutral 2e Lewis base. However, several alternative metal–pyridine interactions have been documented in cases where the metal center is electron rich:

#### Scheme 1



oxidative addition of the aromatic C–H bond of pyridine,<sup>11</sup> η<sup>2</sup>-C,N-<sup>12–16</sup> and η<sup>2</sup>-C,C-coordination modes,<sup>17,18</sup> and single-electron reduction of an η<sup>1</sup>-N-coordinated pyridine.<sup>19</sup>

Here we present a report on the reactivity of C–H bonds in pyridines, both aromatic and benzylic. In contrast to the recently reported Pt case,<sup>20</sup> here we observe not only the activation of the pendant C(sp<sup>2</sup>)–H bonds of substituted pyridines but also activation of C–H bonds on the aliphatic substituents on the pyridine ring and on the pyridine ring itself.<sup>21,22</sup> Our results show that the N-donor site exerts a directing influence on the outcome

<sup>†</sup> Present address: Department of Chemistry, Brandeis University, MS015, Waltham, MA 02454.

- Ozerov, O. V.; Huffman, J. C.; Watson, L. A.; Caulton, K. G. *Organometallics* **2003**, *22*, 2539.
- Ozerov, O. V.; Watson, L. A.; Pink, M.; Caulton, K. G. Manuscript in preparation.
- Chatani, N.; Asaumi, T.; Ikeda, T.; Yorimitsu, S.; Ishii, Y.; Kakiuchi, F.; Murai, S. *J. Am. Chem. Soc.* **2000**, *122*, 12882.
- Chatani, N.; Fukuyama, T.; Tatamidani, H.; Kakiuchi, F.; Murai, S. *J. Org. Chem.* **2000**, *65*, 4039.
- Chatani, N.; Asaumi, T.; Yorimitsu, S.; Ikeda, T.; Kakiuchi, F.; Murai, S. *J. Am. Chem. Soc.* **2001**, *123*, 10935.
- Chatani, N.; Yorimitsu, S.; Asaumi, T.; Kakiuchi, F.; Murai, S. *J. Org. Chem.* **2002**, *67*, 7557.
- Fukuyama, T.; Chatani, N.; Tatsumi, J.; Kakiuchi, F.; Murai, S. *J. Am. Chem. Soc.* **1998**, *120*, 11522.
- Guram, A. S.; Jordan, R. F.; Taylor, D. F. *J. Am. Chem. Soc.* **1991**, *113*, 1833.
- Jordan, R. F.; Taylor, D. F.; Baenziger, N. C. *Organometallics* **1990**, *9*, 1546.
- Kakiuchi, F.; Matsumoto, M.; Sonoda, M.; Fukuyama, T.; Chatani, N.; Murai, S.; Furukawa, N.; Seki, Y. *Chem. Lett.* **2000**, *7*, 750.

- Selnau, H. E.; Merola, J. S. *Organometallics* **1993**, *12*, 1583.
- Smith, D. P.; Strickler, J. R.; Gray, S. D.; Bruck, M. A.; Holmes, R. S.; Wigley, D. E. *Organometallics* **1992**, *11*, 1275.
- Strickler, J. R.; Bruck, M. A.; Wigley, D. E. *J. Am. Chem. Soc.* **1990**, *112*, 2814.
- Neithamer, D. R.; Párkányi, L.; Mitchell, J. F.; Wolczanski, P. T. *J. Am. Chem. Soc.* **1988**, *110*, 4421.
- Kleckley, T. S.; Bennett, J. S.; Wolczanski, P. T.; Lobkovski, E. B. *J. Am. Chem. Soc.* **1997**, *119*, 247.
- Covert, K. J.; Neithamer, D. R.; Zonneville, M. C.; LaPointe, R. E.; Schaller, C. P.; Wolczanski, P. T. *Inorg. Chem.* **1991**, *30*, 2494.
- Meiere, S. H.; Brooks, B. C.; Gunnoe, T. B.; Carrig, E. H.; Sabat, M.; Harman, W. D. *Organometallics* **2001**, *20*, 3661.
- Harman, W. D. *Chem. Rev.* **1997**, *97*, 1953.
- Durfee, L. D.; Hill, J. E.; Kerschner, J. L.; Fanwick, P. E.; Rothwell, I. P. *Inorg. Chem.* **1989**, *28*, 3095.
- Wong-Foy, A. G.; Henlig, L. M.; Day, M.; Labinger, J. A.; Bercaw, J. E. *J. Mol. Catal.* **2002**, *189*, 3.

of the activation of C–H bonds, similar to that observed by others in pyridines and other heterocycles.<sup>3–11,20</sup>

To make the new Re–carbon bonds in the reaction in Scheme 1, the Re center in (PNP)ReH<sub>4</sub>, **1**, has to lose the hydrides, which in this case is accomplished by hydrogenation of excess olefin. To make new Re–C bonds in reactions with substrates that do not possess H<sub>2</sub>-accepting functionalities, a different approach must be taken. Either the formation of new bonds to Re is thermodynamically favorable enough to expel free H<sub>2</sub> or an additional, sacrificial H<sub>2</sub> acceptor must be introduced. We report here examples of both types of behavior, with cyclooctene suitably serving as a sacrificial H<sub>2</sub> acceptor. We also report that the compound (PNP)ReH<sub>2</sub>(cyclooctyne), **2**, incorporating the elements of cyclooctene on a (PNP)Re center, can serve as a source of “naked (PNP)Re” via loss of cyclooctene or, upon hydrogenation, of cyclooctane.

## Experimental Section

**General Considerations.** All manipulations were performed using standard Schlenk techniques or in an argon-filled glovebox unless otherwise noted. Pentane, *neo*-hexane, tetramethylsilane, cyclooctane, cyclohexane, cyclooctene, C<sub>6</sub>D<sub>6</sub>, C<sub>7</sub>D<sub>8</sub>, and C<sub>8</sub>D<sub>12</sub> were vacuum-transferred from NaK/benzophenone/18-crown-6. Hexamethyldisiloxane was distilled from NaK alloy. Substituted pyridines were fractionally distilled from CaH<sub>2</sub>. (PNP<sup>Pr</sup>)ReH<sub>4</sub> (**1**) was prepared by the methodology used to prepare (PNP<sup>Cy</sup>)ReH<sub>4</sub> (Cy = cyclohexyl).<sup>1</sup> Full details will be published in a separate report. <sup>1</sup>H NMR chemical shifts are reported in parts per million relative to protio impurities in the deuterated solvents or by external referencing in protio solvents. <sup>31</sup>P spectra are referenced to external standards of 85% H<sub>3</sub>PO<sub>4</sub> (at 0 ppm). NMR spectra were recorded with a Varian Gemini 2000 (300 MHz <sup>1</sup>H; 121 MHz <sup>31</sup>P; 75 MHz <sup>13</sup>C), a Varian Unity Inova instrument (400 MHz <sup>1</sup>H; 162 MHz <sup>31</sup>P; 101 MHz <sup>13</sup>C), or a Varian Unity Inova instrument (500 MHz <sup>1</sup>H, 126 MHz <sup>13</sup>C). Elemental analyses were performed by CALI, Inc. (Parsippany, NJ).

**(PNP<sup>Pr</sup>)ReH<sub>2</sub>(Cyclooctyne) (2).** (PNP<sup>Pr</sup>)ReH<sub>4</sub> (**1**) (200 mg, 343 μmol) was dissolved in 1 mL of Me<sub>3</sub>SiOSiMe<sub>3</sub> and treated with cyclooctene (0.4 mL, 3.1 mmol). The mixture was kept at 90 °C for 1 h during which time the solution turned light-red. The solution was filtered to remove a minor amount of insolubles and placed in the freezer at –30 °C for 24 h. The pink precipitate was collected by decantation, washed with cold SiMe<sub>4</sub>, and dried in vacuo. Yield: 205 mg (87%). <sup>1</sup>H NMR (C<sub>7</sub>D<sub>8</sub>): δ 3.31 (t, 6 Hz, 4H, cyclooctyne), 2.61 (m, J<sub>HH</sub> = 7 Hz, 2H, PCH), 1.94 (m, J<sub>HH</sub> = 7 Hz, 2H, PCH), 1.79 (br m, 4H, cyclooctyne), 1.48 (AB dvt, J<sub>HH</sub> = 14 Hz, J<sub>HP</sub> = 4 Hz, 2H, PCH<sub>2</sub>Si), 1.37 (br m, 4H, cyclooctyne), 1.21 (overlapping multiplets, 18 H, PCH–CH<sub>3</sub>), 1.13 (apparent q (dvt), 8 Hz, 6H, PCH–CH<sub>3</sub>), 1.09 (AB dvt, J<sub>HH</sub> = 14 Hz, J<sub>HP</sub> = 4 Hz, 2H, PCH<sub>2</sub>Si), 0.31 (s, 6H, SiCH<sub>3</sub>), 0.02 (s, 6H, SiCH<sub>3</sub>), –3.45 (dt, J<sub>HH</sub> = 10 Hz, J<sub>HP</sub> = 30 Hz, 1H, ReH), –6.54 (apparent quartet, J<sub>HH</sub> = 10 Hz, J<sub>HP</sub> = 12 Hz, 1H, ReH). <sup>31</sup>P NMR (C<sub>7</sub>D<sub>8</sub>, –76 °C): δ 54.5 (br), 36.5 (br). <sup>31</sup>P{<sup>1</sup>H} NMR (C<sub>7</sub>D<sub>8</sub>, 22 °C): δ 44.1 (br s). <sup>13</sup>C{<sup>1</sup>H} NMR (C<sub>7</sub>D<sub>8</sub>): δ 190.4 (t, 8 Hz, C≡C of cyclooctyne), 35.7 (s, CH<sub>2</sub> of cyclooctyne), 29.3 (vt, 14 Hz, P–CH), 27.4 (s, CH<sub>2</sub> of cyclooctyne), 26.8 (vt, 10 Hz, P–CH), 26.4 (s, CH<sub>2</sub> of cyclooctyne), 20.4 (s, PCH–CH<sub>3</sub>), 19.6 (s, PCH–CH<sub>3</sub>), 18.8 (s, PCH–CH<sub>3</sub>), 18.5 (s, PCH–CH<sub>3</sub>), 18.1 (br s, PCH<sub>2</sub>Si), 4.8 (s, SiCH<sub>3</sub>), 4.6 (br s, SiCH<sub>3</sub>). Elem. Anal. for C<sub>26</sub>H<sub>58</sub>NP<sub>2</sub>ReSi<sub>2</sub>. Found (Calcd): C, 45.19 (45.32); H, 8.53 (8.48); N, 1.96 (2.03).

Compounds **4** and **5** can be prepared either by reaction of an appropriate pyridine reagent with **2** or with [**1** + 3 equiv of cyclooctene]. Representative detailed descriptions are given below.

**(PNP<sup>Pr</sup>)ReH(4-Methyl-2-pyridyl) (4a).** (PNP<sup>Pr</sup>)ReH<sub>2</sub>(cyclooctyne) (50 mg, 72 μmol) was dissolved in 0.6 mL of cyclooctane, and 4-methylpyridine (30 μL, 310 μmol) was added. This mixture was heated for 15 min at 110 °C. <sup>31</sup>P NMR showed >99% conversion to the product. The volatiles were removed in vacuo, leaving a bright-red oil. C<sub>30</sub>H<sub>56</sub>N<sub>3</sub>P<sub>2</sub>ReSi<sub>2</sub>. Calcd (Found): C, 47.22 (47.31); H, 7.40 (7.25); N, 5.51 (5.55). <sup>1</sup>H NMR (C<sub>6</sub>D<sub>6</sub>): δ 7.15 (d, 1H, 8 Hz, arom CH), 6.42 (s, 1H, arom CH), 5.30 (d, 1H, 8 Hz, arom CH), 1.77 (s, 3H, pyridyl-CH<sub>3</sub>), 1.74 (m, 4H, PCH), 1.15 (apparent q (dvt), 8 Hz, 6H, PCH–CH<sub>3</sub>), 1.00 (apparent q (dvt), 8 Hz, 6H, PCH–CH<sub>3</sub>), 0.94 (apparent q (dvt), 8 Hz, 6H, PCH–CH<sub>3</sub>), 0.88 (apparent q (dvt), 8 Hz, 6H, PCH–CH<sub>3</sub>), 0.72 (AB dvt, J<sub>HH</sub> = 15 Hz, J<sub>HP</sub> = 4 Hz, 2H, PCH<sub>2</sub>Si), 0.67 (AB dvt, J<sub>HH</sub> = 15 Hz, J<sub>HP</sub> = 4 Hz, 2H, PCH<sub>2</sub>Si), 0.37 (s, 6H, SiCH<sub>3</sub>), 0.36 (s, 6H, SiCH<sub>3</sub>), –3.91 (t, 13 Hz, 1H, ReH). <sup>31</sup>P{<sup>1</sup>H} NMR (C<sub>6</sub>D<sub>6</sub>): δ 34.8 (s). <sup>13</sup>C{<sup>1</sup>H} NMR (C<sub>6</sub>D<sub>6</sub>): δ 170.5 (t, 6 Hz, Re–C), 143.2 (s, arom C–Me), 139.1 (s, arom CH), 128.2 (s, arom CH), 113.6 (s, arom CH), 31.1 (t, 12 Hz, P–CH), 24.1 (t, 9 Hz, P–CH), 20.9 (s, pyridyl-CH<sub>3</sub>), 19.8 (s, PCH–CH<sub>3</sub>), 19.4 (s, PCH–CH<sub>3</sub>), 18.1 (s, PCH–CH<sub>3</sub>), 16.6 (s, PCH–CH<sub>3</sub>), 13.5 (s, PCH<sub>2</sub>Si), 6.3 (s, SiCH<sub>3</sub>), 6.2 (t, 2 Hz, SiCH<sub>3</sub>). Elem. Anal. for (C<sub>24</sub>H<sub>51</sub>N<sub>2</sub>P<sub>2</sub>ReSi<sub>2</sub>). Calcd (Found): C, 42.90 (43.02); H, 7.65 (7.78); N, 4.17 (4.19).

**(PNP<sup>Pr</sup>)ReH(4-*t*-Butyl-2-pyridyl) (4b).** **4b** was observed in situ during thermolyses of **2** in the presence of **3b**. <sup>1</sup>H NMR (4-*tert*-butylpyridine/cyclo-C<sub>6</sub>H<sub>12</sub>): δ –3.85 (t, 13 Hz, 1H, ReH). <sup>31</sup>P{<sup>1</sup>H} NMR (4-*tert*-butylpyridine/cyclo-C<sub>6</sub>H<sub>12</sub>): δ 35.3 (s).

**(PNP<sup>Pr</sup>)ReH(6-Ethyl-2-pyridyl) (4c).** (PNP<sup>Pr</sup>)ReH<sub>2</sub>(Cyclooctyne) (25 mg, 36 μmol) was dissolved in 0.6 mL of 2-ethylpyridine and heated for 10 h at 110 °C. The volatiles were removed in vacuo, leaving a bright-red oil. Attempts to obtain the product in the solid state by crystallization failed. The crude product, however, appears to be analytically pure as indicated by NMR. <sup>1</sup>H NMR (C<sub>6</sub>D<sub>6</sub>): δ 6.54 (d, 1H, 8 Hz, arom CH), 6.49 (t, 1H, 8 Hz, arom CH), 5.45 (d, 1H, 8 Hz, arom CH), 2.43 (q, 7 Hz, 2H, CH<sub>2</sub>CH<sub>3</sub>), 1.77 (m, J<sub>HH</sub> = 7 Hz, 2H, PCH), 1.70 (m, J<sub>HH</sub> = 7 Hz, 2H, PCH), 1.10 (t, 7 Hz, 3H, CH<sub>2</sub>CH<sub>3</sub>), 1.09 (apparent q (dvt), 8 Hz, 6H, PCH–CH<sub>3</sub>), 1.03 (apparent q (dvt), 8 Hz, 6H, PCH–CH<sub>3</sub>), 0.89 (apparent q (dvt), 8 Hz, 6H, PCH–CH<sub>3</sub>), 0.87 (apparent q (dvt), 8 Hz, 6H, PCH–CH<sub>3</sub>), 0.69 (AB dvt, J<sub>HH</sub> = 15 Hz, J<sub>HP</sub> = 4 Hz, 2H, PCH<sub>2</sub>Si), 0.66 (AB dvt, J<sub>HH</sub> = 15 Hz, J<sub>HP</sub> = 4 Hz, 2H, PCH<sub>2</sub>Si), 0.37 (broad (2 overlapping singlets), 12H, SiCH<sub>3</sub>), –3.73 (t, 13 Hz, 1H, ReH). <sup>31</sup>P{<sup>1</sup>H} NMR (C<sub>6</sub>D<sub>6</sub>): δ 33.9 (s). <sup>13</sup>C{<sup>1</sup>H} NMR (C<sub>6</sub>D<sub>6</sub>): δ 169.0 (t, 6 Hz, Re–C), 151.3 (s, arom C–Et), 133.8 (s, arom CH), 125.6 (s, arom CH), 111.6 (s, arom CH), 30.3 (t, 12 Hz, P–CH), 27.9 (s, CH<sub>2</sub>CH<sub>3</sub>), 25.1 (t, 9 Hz, P–CH), 19.4 (s, PCH–CH<sub>3</sub>), 19.2 (s, PCH–CH<sub>3</sub>), 18.5 (s, PCH–CH<sub>3</sub>), 16.9 (s, PCH–CH<sub>3</sub>), 13.3 (s, PCH<sub>2</sub>Si), 12.4 (s, CH<sub>2</sub>CH<sub>3</sub>), 6.4 (s, SiCH<sub>3</sub>), 6.1 (t, 2 Hz, SiCH<sub>3</sub>).

**(PNP<sup>Pr</sup>)Re(4-Methyl-2-pyridyl)<sub>2</sub> (5a).** (PNP<sup>Pr</sup>)ReH<sub>4</sub> (20 mg, 34 μmol) and cyclooctene (15 μL, 113 μmol) were dissolved in 0.6 mL 4-methylpyridine and heated for 10 h at 110 °C. The volatiles were removed in vacuo, leaving an orange solid, pure as indicated by NMR. Recrystallization from pentane yielded 19 mg (73%) of product as a mixture of isomers (4:1 ratio at 22 °C). **Major Isomer.** <sup>1</sup>H NMR (C<sub>6</sub>D<sub>6</sub>): δ 7.60 (d, 2H, 4 Hz, arom CH), 6.63 (s, 2H, arom CH), 5.51 (d, 2H, 4 Hz, arom CH), 1.73 (s, 6H, pyridyl-CH<sub>3</sub>), 1.40 (m, J<sub>HH</sub> = 7 Hz, 4H, PCH), 0.96 (apparent q (dvt), 8 Hz, 12H, PCH–CH<sub>3</sub>), 0.93 (t, J<sub>HP</sub> = 4 Hz, 4H, PCH<sub>2</sub>Si), 0.73 (apparent q (dvt), 8 Hz, 12H, PCH–CH<sub>3</sub>), 0.60 (s, 12H, SiCH<sub>3</sub>). <sup>31</sup>P{<sup>1</sup>H} NMR (C<sub>6</sub>D<sub>6</sub>): δ 20.5 (s). <sup>13</sup>C{<sup>1</sup>H} NMR (C<sub>6</sub>D<sub>6</sub>): δ 181.3 (t, 6 Hz, Re–C), 143.1 (s, arom C–Me), 140.8 (s, arom CH), 125.0 (s, arom CH), 116.7 (s, arom CH), 25.1 (t, 10 Hz, P–CH), 21.2 (s, pyridyl-CH<sub>3</sub>), 18.5 (s, PCH–CH<sub>3</sub>), 17.6 (s, PCH–CH<sub>3</sub>), 14.2 (s, PCH<sub>2</sub>Si), 6.1 (s, SiCH<sub>3</sub>). **Minor Isomer.** <sup>1</sup>H NMR (C<sub>6</sub>D<sub>6</sub>, selected resonances): δ 7.90 (d, 1H, 4 Hz, arom CH), 7.65 (d, 1H, 4 Hz, arom CH), 7.25 (s, 1H, arom CH), 6.34 (s, 1H, arom CH), 5.73 (d, 1H, 4 Hz, arom CH), 5.59 (d, 1H, 4 Hz, arom CH), 1.97 (s, 3H, pyridyl-CH<sub>3</sub>), 1.67 (s, 3H, pyridyl-CH<sub>3</sub>), 0.65 (s, 6H, SiCH<sub>3</sub>), 0.51 (s, 6H, SiCH<sub>3</sub>). <sup>31</sup>P{<sup>1</sup>H} NMR (C<sub>6</sub>D<sub>6</sub>): δ 20.9 (s). <sup>13</sup>C{<sup>1</sup>H} NMR (C<sub>6</sub>D<sub>6</sub>): δ 203.3 (t, 6 Hz, Re–C), 175.3 (t, 6 Hz, Re–C), 143.3 (s, arom C–Me),

(21) Cauty, A. J.; Patel, J.; Skelton, B. W.; White, A. H. *J. Organomet. Chem.* **2000**, *607*, 194.

(22) Retboll, M.; Ishii, Y.; Hidai, M. *Chem. Lett.* **1998**, *12*, 1217.

142.9 (s, arom C-Me), 141.1 (s, arom CH), 140.6 (s, arom CH), 125.6 (s, arom CH), 124.5 (s, arom CH), 117.6 (s, arom CH), 114.2 (s, arom CH), 26.5 (t, 9 Hz, P-CH), 26.1 (t, 10 Hz, P-CH), 21.23 (s, pyridyl-CH<sub>3</sub>), 21.19 (s, pyridyl-CH<sub>3</sub>), 18.5 (s, PCH-CH<sub>3</sub>), 18.4 (s, PCH-CH<sub>3</sub>), 18.04 (s, PCH-CH<sub>3</sub>), 17.95 (s, PCH-CH<sub>3</sub>), 14.4 (s, PCH<sub>2</sub>Si), 6.3 (s, SiCH<sub>3</sub>), 4.5 (s, SiCH<sub>3</sub>). Elem. Anal. for (C<sub>30</sub>H<sub>56</sub>N<sub>3</sub>P<sub>2</sub>ReSi<sub>2</sub>). Calcd (Found): C, 47.22 (47.31); H, 7.40 (7.25); N, 5.51 (5.55).

**(PNP<sup>Pr</sup>)Re(4-*t*-Butyl-2-pyridyl)<sub>2</sub> (5b).** (PNP<sup>Pr</sup>)ReH<sub>4</sub> (30 mg, 51 μmol) and cyclooctene (23 μL, 173 μmol) were dissolved in 0.5 mL cyclohexane, and 4-*tert*-butylpyridine (0.1 mL) was added to it. This mixture was heated at 110 °C while being monitored by NMR periodically. After 5 days, the conversion to the product is >99% complete. The volatiles were removed in vacuo at 90 °C, leaving an orange solid, pure as indicated by NMR. The high solubility of the compound makes recrystallization an inadequate purification method; however, the crude product was 99% pure as indicated by NMR. The product exists as a mixture of isomers (5:1 ratio at 22 °C). **Major Isomer.** <sup>1</sup>H NMR (C<sub>6</sub>D<sub>6</sub>): δ 7.64 (d, 2H, 4 Hz, arom CH), 6.91 (s, 2H, arom CH), 5.69 (d, 2H, 4 Hz, arom CH), 1.17 (s, 18H, pyridyl-CMe<sub>3</sub>), 1.43 (m, J<sub>HH</sub> = 7 Hz, 4H, PCH), 0.99 (apparent q (dvt), 8 Hz, 12H, PCH-CH<sub>3</sub>), 0.96 (t, J<sub>HP</sub> = 4 Hz, 4H, PCH<sub>2</sub>Si), 0.73 (apparent q (dvt), 8 Hz, 12H, PCH-CH<sub>3</sub>), 0.63 (s, 12H, SiCH<sub>3</sub>). <sup>31</sup>P{<sup>1</sup>H} NMR (C<sub>6</sub>D<sub>6</sub>): δ 19.5 (s). <sup>13</sup>C{<sup>1</sup>H} NMR (C<sub>6</sub>D<sub>6</sub>): δ 179.9 (t, 6 Hz, Re-C), 156.1 (s, arom C-CMe<sub>3</sub>), 140.9 (s, arom CH), 121.6 (s, arom CH), 113.0 (s, arom CH), 34.5 (s, CMe<sub>3</sub>), 30.2 (s, pyridyl-C(CH<sub>3</sub>)), 25.2 (t, 10 Hz, P-CH), 18.5 (s, PCH-CH<sub>3</sub>), 17.8 (s, PCH-CH<sub>3</sub>), 14.8 (s, PCH<sub>2</sub>Si), 6.1 (s, SiCH<sub>3</sub>). **Minor Isomer.** <sup>1</sup>H NMR (C<sub>6</sub>D<sub>6</sub>, selected resonances): δ 8.00 (d, 1H, 4 Hz, arom CH), 7.79 (d, 1H, 4 Hz, arom CH), 7.54 (s, 1H, arom CH), 6.59 (s, 1H, arom CH), 5.94 (d, 1H, 4 Hz, arom CH), 5.77 (d, 1H, 4 Hz, arom CH), 1.32 (s, 9H, pyridyl-CMe<sub>3</sub>), 1.14 (s, 9H, pyridyl-CMe<sub>3</sub>), 0.66 (s, 6H, SiCH<sub>3</sub>), 0.54 (s, 6H, SiCH<sub>3</sub>). <sup>31</sup>P{<sup>1</sup>H} NMR (C<sub>6</sub>D<sub>6</sub>): δ 20.4 (s). <sup>13</sup>C{<sup>1</sup>H} NMR (C<sub>6</sub>D<sub>6</sub>): δ 203.9 (t, 6 Hz, Re-C), 175.2 (t, 6 Hz, Re-C), 156.5 (s, arom C-CMe<sub>3</sub>), 155.5 (s, arom C-CMe<sub>3</sub>), 141.5 (s, arom CH), 140.6 (s, arom CH), 125.9 (s, arom CH), 122.6 (s, arom CH), 113.6 (s, arom CH), 110.2 (s, arom CH), 34.4 (s, CMe<sub>3</sub>), 34.3 (s, CMe<sub>3</sub>), 30.7 (s, pyridyl-C(CH<sub>3</sub>)), 30.1 (s, pyridyl-C(CH<sub>3</sub>)), 26.8 (t, 9 Hz, P-CH), 26.1 (t, 10 Hz, P-CH), 18.5 (s, PCH-CH<sub>3</sub>), 18.3 (s, PCH-CH<sub>3</sub>), 17.9 (s, PCH-CH<sub>3</sub>), 17.8 (s, PCH-CH<sub>3</sub>), 14.3 (s, PCH<sub>2</sub>Si), 6.3 (s, SiCH<sub>3</sub>), 4.3 (s, SiCH<sub>3</sub>).

**(PNP<sup>Pr</sup>)ReH<sub>3</sub>(4-Methyl-2-pyridyl) (6a).** (PNP<sup>Pr</sup>)ReH(4-methyl-2-pyridyl) (32 mg, 47 μmol) was dissolved in 0.6 mL of C<sub>6</sub>D<sub>6</sub> in a J. Young tube. This solution was degassed, and the headspace of the NMR tube was filled with 405 Torr of H<sub>2</sub> (approximate volume 2 mL, ca. 48 μmol). After 20 min, a mixture containing of **6a** (55%), **4a** (30%), and **1** (15%) formed. The <sup>31</sup>P NMR peak of **1** was very broad, presumably because of slow equilibrium with its adduct with 4-methylpyridine (liberated by hydrogenation of **6a**). <sup>1</sup>H NMR (C<sub>6</sub>D<sub>6</sub>): δ 7.77 (d, 1H, 8 Hz, arom CH), 6.55 (s, 1H, arom CH), 5.63 (d, 1H, 8 Hz, arom CH), 1.74 (s, 3H, pyridyl-CH<sub>3</sub>), 1.87 (m, 2H, PCH), 1.47 (m, 2H, PCH), 1.15 (two overlapping apparent q (dvt), 12H, PCH-CH<sub>3</sub>), 1.09 (apparent q (dvt), 8 Hz, 6H, PCH-CH<sub>3</sub>), 0.74 (apparent q (dvt), 8 Hz, 6H, PCH-CH<sub>3</sub>), 0.53 (s, 6H, SiCH<sub>3</sub>), 0.43 (s, 6H, SiCH<sub>3</sub>), -5.44 (t, 22 Hz, 3H, ReH<sub>3</sub>), the P-CH<sub>2</sub>-Si signals were obscured by other signals in this mixture. <sup>31</sup>P{<sup>1</sup>H} NMR (C<sub>6</sub>D<sub>6</sub>): δ 48.7 (s). <sup>13</sup>C{<sup>1</sup>H} NMR (C<sub>6</sub>D<sub>6</sub>, selected resonances): δ 184.9 (t, 6 Hz, Re-C), 28.8 (t, 12 Hz, P-CH), 26.2 (t, 10 Hz, P-CH), 20.8 (s, pyridyl-CH<sub>3</sub>), 19.6 (s, PCH-CH<sub>3</sub>), 18.6 (s, PCH-CH<sub>3</sub>), 18.4 (s, PCH-CH<sub>3</sub>), 17.5 (s, PCH-CH<sub>3</sub>), 12.2 (s, PCH<sub>2</sub>Si), 5.7 (s, SiCH<sub>3</sub>), 4.3 (t, 2 Hz, SiCH<sub>3</sub>).

**(PNP<sup>Pr</sup>)ReH<sub>3</sub>(4-*t*-Butyl-2-pyridyl) (6b) and (PNP<sup>Pr</sup>)ReH<sub>3</sub>(6-Ethyl-2-pyridyl) (6c).** **6b** and **6c** can be observed in situ upon thermolysis of **2** in **3a-c**, respectively. <sup>31</sup>P NMR for **6b** (4-*tert*-butylpyridine/cyclo-C<sub>6</sub>H<sub>12</sub>): δ 49.0. <sup>31</sup>P NMR for **6c** (2-ethylpyridine): δ 51.6.

**(PNP<sup>Pr</sup>)ReH(≡C-(6-Methyl-2-pyridyl)) (7a).** (PNP<sup>Pr</sup>)ReH<sub>2</sub>(cyclooctyne) (25 mg, 36 μmol) was dissolved in 0.6 mL of cyclooctane, and 0.1 mL of 2,6-dimethylpyridine was added to the mixture. It was heated for 30 min at 110 °C. The volatiles were removed in vacuo,

leaving behind a brown-red oil. Attempts to obtain the product in the solid state by crystallization failed. The crude product appears to be analytically pure as indicated by NMR. <sup>1</sup>H NMR (C<sub>6</sub>D<sub>6</sub>): δ 7.03 (d, 1H, 8 Hz, arom CH), 6.94 (t, 1H, 8 Hz, arom CH), 6.66 (d, 1H, 8 Hz, arom CH), 2.39 (m, J<sub>HH</sub> = 7 Hz, 2H, PCH), 2.35 (s, 3H, pyridyl-CH<sub>3</sub>), 1.88 (m, J<sub>HH</sub> = 7 Hz, 2H, PCH), 1.33 (apparent q (dvt), 8 Hz, 6H, PCH-CH<sub>3</sub>), 1.24 (apparent q (dvt), 8 Hz, 6H, PCH-CH<sub>3</sub>), 1.10 (apparent q (dvt), 8 Hz, 6H, PCH-CH<sub>3</sub>), 1.05 (apparent q (dvt), 8 Hz, 6H, PCH-CH<sub>3</sub>), 0.90 (AB dvt, J<sub>HH</sub> = 15 Hz, J<sub>HP</sub> = 4 Hz, 2H, PCH<sub>2</sub>Si), 0.82 (AB dvt, J<sub>HH</sub> = 15 Hz, J<sub>HP</sub> = 4 Hz, 2H, PCH<sub>2</sub>Si), 0.42 (s, 6H, SiCH<sub>3</sub>), 0.32 (s, 6H, SiCH<sub>3</sub>), -9.16 (t, 15 Hz, 1H, ReH). <sup>31</sup>P{<sup>1</sup>H} NMR (C<sub>6</sub>D<sub>6</sub>): δ 59.0 (s). <sup>13</sup>C{<sup>1</sup>H} NMR (C<sub>6</sub>D<sub>6</sub>): δ 269.3 (t, 12 Hz, Re≡C), 168.3 (br s, arom C), 158.0 (s, arom C), 135.3 (s, arom CH), 119.6 (s, arom CH), 118.9 (s, arom CH), 29.8 (t, 13 Hz, P-CH), 29.6 (t, 10 Hz, P-CH), 24.7 (s, CH<sub>2</sub>CH<sub>3</sub>), 20.5 (s, PCH-CH<sub>3</sub>), 19.1 (s, PCH-CH<sub>3</sub>), 18.9 (s, PCH-CH<sub>3</sub>), 17.5 (s, PCH-CH<sub>3</sub>), 10.1 (s, PCH<sub>2</sub>Si), 7.3 (s, SiCH<sub>3</sub>), 6.4 (t, 2 Hz, SiCH<sub>3</sub>).

**(PNP<sup>Pr</sup>)ReH(≡C-(4,6-Dimethyl-2-pyridyl)) (7b).** (PNP<sup>Pr</sup>)ReH<sub>2</sub>(cyclooctyne) (25 mg, 36 μmol) was dissolved in 0.6 mL of cyclooctane, and 0.1 mL 2,4,6-trimethylpyridine was added to the mixture. It was heated for 30 min at 110 °C. The volatiles were removed in vacuo, leaving behind a brown-red oil. Attempts to obtain the product in solid state by crystallization failed. The crude product appears to be analytically pure by NMR. <sup>1</sup>H NMR (C<sub>6</sub>D<sub>6</sub>): δ 6.51 (s, 1H, arom CH), 6.43 (s, 1H, arom CH), 2.43 (s, 3H, pyridyl-CH<sub>3</sub>), 2.40 (m, J<sub>HH</sub> = 7 Hz, 2H, PCH), 2.37 (s, 3H, pyridyl-CH<sub>3</sub>), 1.89 (m, J<sub>HH</sub> = 7 Hz, 2H, PCH), 1.36 (apparent q (dvt), 8 Hz, 6H, PCH-CH<sub>3</sub>), 1.26 (apparent q (dvt), 8 Hz, 6H, PCH-CH<sub>3</sub>), 1.11 (apparent q (dvt), 8 Hz, 6H, PCH-CH<sub>3</sub>), 1.06 (apparent q (dvt), 8 Hz, 6H, PCH-CH<sub>3</sub>), 0.91 (AB dvt, J<sub>HH</sub> = 15 Hz, J<sub>HP</sub> = 4 Hz, 2H, PCH<sub>2</sub>Si), 0.84 (AB dvt, J<sub>HH</sub> = 15 Hz, J<sub>HP</sub> = 4 Hz, 2H, PCH<sub>2</sub>Si), 0.43 (s, 6H, SiCH<sub>3</sub>), 0.32 (s, 6H, SiCH<sub>3</sub>), -9.26 (t, 15 Hz, 1H, ReH). <sup>31</sup>P{<sup>1</sup>H} NMR (C<sub>6</sub>D<sub>6</sub>): δ 59.1 (s). <sup>13</sup>C{<sup>1</sup>H} NMR (C<sub>6</sub>D<sub>6</sub>): δ 269.8 (t, 12 Hz, Re≡C), 168.2 (br s, arom C), 157.8 (s, arom C), 146.0 (s, arom C), 120.5 (s, arom CH), 120.3 (s, arom CH), 29.8 (t, 13 Hz, P-CH), 29.6 (t, 10 Hz, P-CH), 24.5 (s, pyridyl-CH<sub>3</sub>), 20.5 (s, PCH-CH<sub>3</sub>), 20.4 (s, pyridyl-CH<sub>3</sub>), 19.2 (s, PCH-CH<sub>3</sub>), 18.9 (s, PCH-CH<sub>3</sub>), 17.5 (s, PCH-CH<sub>3</sub>), 10.2 (s, PCH<sub>2</sub>Si), 7.3 (s, SiCH<sub>3</sub>), 6.4 (t, 2 Hz, SiCH<sub>3</sub>).

**(PNP<sup>Pr</sup>)ReH(Pyridylvinyl) (8).** (PNP<sup>Pr</sup>)ReH<sub>4</sub> (25 mg, 43 μmol) was dissolved in 0.3 mL of hexamethyldisiloxane, and 2-vinylpyridine (14.0 μL, 130 μmol) was added to the mixture. Overnight and at ambient temperature, dark-brown crystals formed and were collected by decantation, washed with cold SiMe<sub>4</sub>, and dried. Yield: 21 mg (72%). When this reaction was performed in an NMR tube, NMR indicated a quantitative conversion to **8** in <30 min. <sup>1</sup>H NMR (C<sub>6</sub>D<sub>6</sub>): δ 11.31 (dd, 4 Hz, 6 Hz, 1H, α-vinyl CH), 8.83 (d, 1H, 5 Hz, ortho-CH), 7.50 (d, 4 Hz, 6 Hz, 1H, β-vinyl CH), 7.08 (d, 1H, 4 Hz, para-CH), 6.67 (t, 6 Hz, 1H, meta-CH), 5.93 (t, 6 Hz, 1H, meta-CH), 1.88 (m, J<sub>HH</sub> = 7 Hz, 2H, PCH), 1.78 (m, J<sub>HH</sub> = 7 Hz, 2H, PCH), 0.91 (apparent q (dvt), 8 Hz, 6H, PCH-CH<sub>3</sub>), 0.85 (apparent q (dvt), 8 Hz, 6H, PCH-CH<sub>3</sub>), 0.83 (apparent q (dvt), 8 Hz, 6H, PCH-CH<sub>3</sub>), 0.72 (AB dvt, J<sub>HH</sub> = 15 Hz, J<sub>HP</sub> = 4 Hz, 2H, PCH<sub>2</sub>Si), 0.63 (apparent q (dvt), 8 Hz, 6H, PCH-CH<sub>3</sub>), 0.42 (s, 6H, SiCH<sub>3</sub>), 0.39 (s, 6H, SiCH<sub>3</sub>), 0.36 (AB dvt, J<sub>HH</sub> = 15 Hz, J<sub>HP</sub> = 4 Hz, 2H, PCH<sub>2</sub>Si), -5.26 (td, J<sub>HP</sub> = 13 Hz, J<sub>HH</sub> = 4 Hz, 1H, ReH). <sup>31</sup>P{<sup>1</sup>H} NMR (C<sub>6</sub>D<sub>6</sub>): δ 20.4 (s). <sup>13</sup>C{<sup>1</sup>H} NMR (C<sub>6</sub>D<sub>6</sub>): δ 234.9 (t, 6 Hz, Re-CH), 163.6 (s), 157.2 (s), 131.7 (s), 117.9 (s), 114.5 (s), 111.7 (s), 28.7 (t, 12 Hz, P-CH), 28.1 (t, 10 Hz, P-CH), 18.3 (s, PCH-CH<sub>3</sub>), 17.59 (s, PCH-CH<sub>3</sub>), 17.43 (s, PCH-CH<sub>3</sub>), 17.39 (s, PCH-CH<sub>3</sub>), 11.6 (s, PCH<sub>2</sub>Si), 6.3 (s, SiCH<sub>3</sub>), 5.2 (s, SiCH<sub>3</sub>).

## Computational Details

All calculations were performed with the Gaussian 98 package<sup>23</sup> at the B3PW91<sup>24-27</sup> level of theory. Basis sets used included LANL2DZ for Re and Si, 6-31G\* for C and N, and 6-31G\*\* for all hydrogens.<sup>28</sup> The basis set LANL2DZ is the Los Alamos National Laboratory ECP plus a double-ζ valence on Re, P, and Si;<sup>29-31</sup> additional d polarization

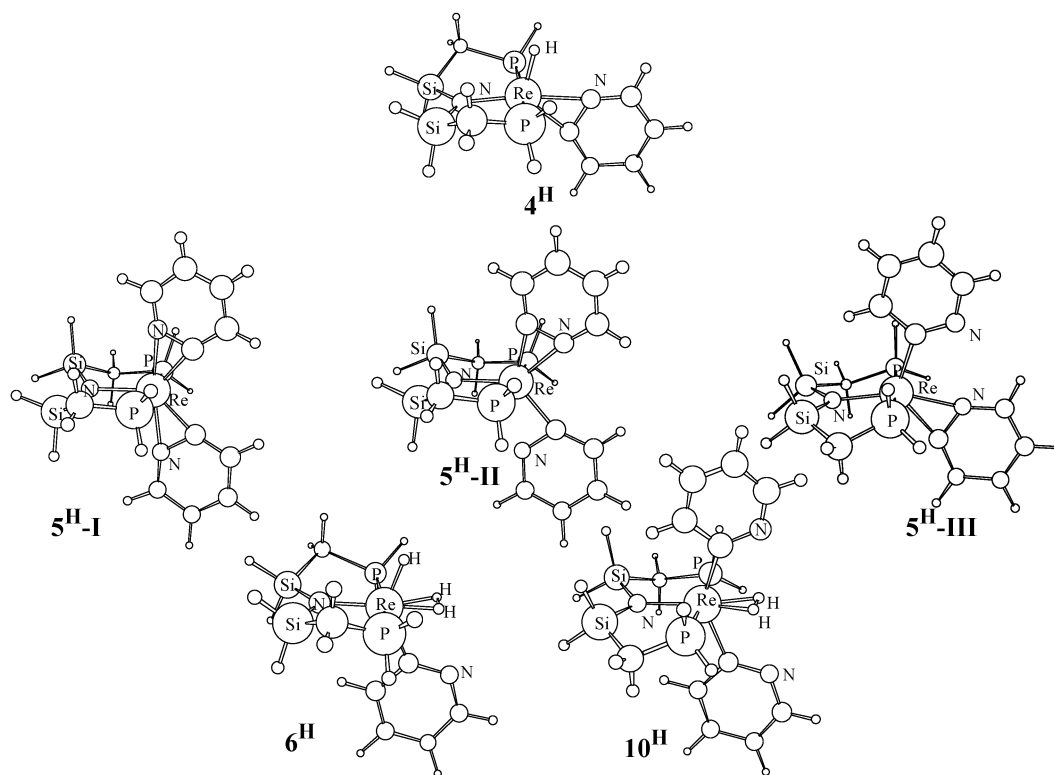


**Figure 1.** DFT-optimized structures of pyridyl complexes. Unlabeled circles are carbon (large) or hydrogen (small).

functions<sup>32</sup> were added to all phosphorus and silicon atoms in all DFT calculations. All optimizations were performed with  $C_1$  symmetry, and all minima were confirmed by analytical calculation of frequencies, which were also used to compute zero point energy corrections without scaling.

The initial geometries of **4<sup>H</sup>** and **5<sup>H</sup>-I** were adapted from refined crystal structures of the analogous compounds, with all silicon methyl and phosphorus isopropyl groups replaced by hydrogen. All other initial geometries for the Re–PNP core in the optimization of (PNP)ReH<sub>m</sub>L<sub>m</sub> species were taken from the optimized geometry of the Re–PNP core of (PNP)ReH<sub>4</sub>. The starting structures of **6<sup>H</sup>** and **10<sup>H</sup>** were thus trihydride and dihydride (not dihydrogen), respectively, with all hydrides coplanar and the Re/H plane perpendicular to the Re/P plane. Regardless of the nature of the hydrogen ligands employed in the initial geometry or their rotational conformation, each starting structure converged to that reported in Figure 1.

### X-ray Structure Determination

**(a) General.** Data for all compounds were collected using a Bruker SMART6000 system. A suitable crystal was placed onto the tip of a 0.1 mm diameter glass capillary and mounted on the goniostat at 120 K. The data collection was carried out using Mo K $\alpha$  radiation (graphite monochromator) and a detector distance of 5.0 cm. The intensity data were corrected for absorption (SADABS).<sup>33</sup> Final cell constants were calculated from the xyz centroids of strong reflections from the actual data collection after integration.<sup>34</sup> The space groups were determined on the basis of systematic absences and intensity statistics. The structures were solved with direct methods<sup>35</sup> and refined with full-matrix least squares.<sup>36</sup> All non-hydrogen atoms were refined with anisotropic displacement parameters. The hydrogen atoms were placed in ideal positions and refined as riding atoms with individual or relative isotropic displacement parameters, except for metal-bonded hydrogen atoms for which all parameters were refined. Remaining electron densities are within the expected range and located in the vicinity of the metal atoms. Details are listed in Table 1.

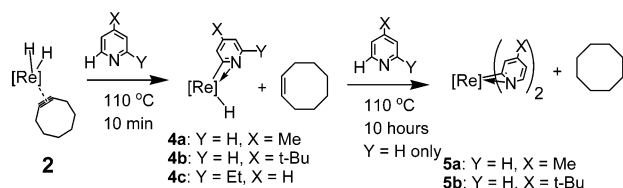
**(b) 4a.** The asymmetric unit contains half of a formula unit. Rhenium, N1, H1r, and the pyridine are located on special positions (mirror at 0,  $1/2$ , 0). Si1, C1, C2, C3, P1, and one *i*-propyl group are disordered over two positions with site occupancies set to be 50:50. Chemically equivalent distances were restrained to be similar within an effective standard deviation.

**(c) 5a.** There are two independent half molecules per asymmetric unit. Re and N1 of each molecule are located on special positions (two 2-folds at 0,  $y$ ,  $1/4$  and  $1/2$ ,  $y$ ,  $1/4$ ). One of the *i*-propyl groups in one molecule is disordered over two positions (70:30).

- (23) Frisch, M. J.; Trucks, G. W.; Schlegel, H. B.; Scuseria, G. E.; Robb, M. A.; Cheeseman, J. R.; Zakrzewski, V. G.; Montgomery, J. A., Jr.; Stratmann, R. E.; Burant, J. C.; Dapprich, S.; Millam, J. M.; Daniels, A. D.; Kudin, K. N.; Strain, M. C.; Farkas, O.; Tomasi, J.; Barone, V.; Cossi, M.; Cammi, R.; Mennucci, B.; Pomelli, C.; Adamo, C.; Clifford, S.; Ochterski, J.; Petersson, G. A.; Ayala, P. Y.; Cui, Q.; Morokuma, K.; Malick, D. K.; Rabuck, A. D.; Raghavachari, K.; Foresman, J. B.; Cioslowski, J.; Ortiz, J. V.; Stefanov, B. B.; Liu, G.; Liashenko, A.; Piskorz, P.; Komaromi, I.; Gomperts, R.; Martin, R. L.; Fox, D. J.; Keith, T.; Al-Laham, M. A.; Peng, C. Y.; Nanayakkara, A.; Gonzalez, C.; Challacombe, M.; Gill, P. M. W.; Johnson, B. G.; Chen, W.; Wong, M. W.; Andres, J. L.; Head-Gordon, M.; Replogle, E. S.; Pople, J. A. *Gaussian 98*; Gaussian, Inc.: Pittsburgh, PA, 1998.
- (24) Becke, A. D. *Phys. Rev.* **1988**, *A38*, 3098.
- (25) Becke, A. D. *J. Chem. Phys.* **1993**, *98*, 1372.
- (26) Becke, A. D. *J. Chem. Phys.* **1993**, *98*, 5648.
- (27) Perdue, J. P.; Wang, Y. *Phys. Rev.* **1991**, *45*, 13244.
- (28) Hariharan, P. C.; Pople, J. A. *Theor. Chim. Acta* **1973**, *28*, 213.
- (29) Hay, P. J.; Wadt, W. R. *J. Chem. Phys.* **1985**, *82*, 270.
- (30) Hay, P. J.; Wadt, W. R. *J. Chem. Phys.* **1985**, *82*, 299.
- (31) Wadt, W. R.; Hay, P. J. *J. Chem. Phys.* **1985**, *82*, 284.
- (32) Hollwarth, A.; Bohme, M.; Dapprich, S.; Ehlers, A. W.; Gobbi, A.; Jonas, V.; Kohler, K. F.; Stegmann, R.; Veldkamp, A.; Frenking, G. *Chem. Phys. Lett.* **1993**, *208*, 237.

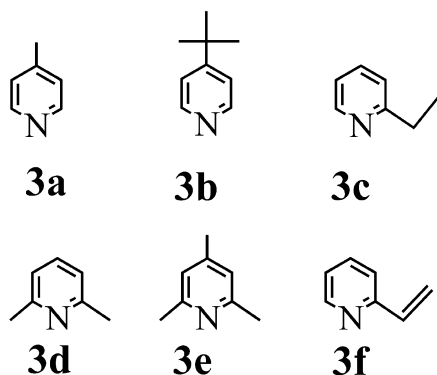
- (33) Blessing, R. *Acta Crystallogr.* **1995**, *A51*, 33.
- (34) *SAINT 6.1*; Bruker Analytical X-ray Systems: Madison, WI.
- (35) Altomare, A.; Cascarno, G.; Giacovazzo, C.; Gualardi, A. *J. Appl. Crystallogr.* **1993**, *26*, 343.
- (36) *SHELXTL-Plus V5.10*; Bruker Analytical Systems: Madison, WI.

## Scheme 2



## Results

Thermolysis (110 °C, cyclohexane or cyclooctane solvent) of (PNP)ReH<sub>2</sub>(cyclooctyne) (**2**) (Scheme 1) in the presence of  $\geq 1$  equiv of any of **3a–c** initially (10 min) produces (PNP)ReH(pyridyl) (**4a–c**) (Scheme 2). In the formation of **4a–c**, 1 equiv of cyclooctene is produced, as identified by NMR. Compounds **4a–c** are characterized by a single resonance at ca. 34 ppm in <sup>31</sup>P NMR, a hydridic resonance at ca. –3.8 ppm in <sup>1</sup>H NMR, and a triplet signal for C<sub>α</sub> at ca. 170 ppm in <sup>13</sup>C NMR. Overall, the NMR spectra of compounds **4a–c** are those of species of C<sub>s</sub> symmetry, consistent with the plane of the pyridine ring being perpendicular to the time-averaged plane of the PNP ligand. The hapticity of the pyridyl ligand could not be discerned from these spectra.



If the reaction mixture containing excess **3a,b** and the in situ formed **4a,b** is kept at 110 °C for an extended period of time (>10 h), a quantitative conversion to **5a,b** is observed along with production of cyclooctane. Both the rate of formation of **5** from **4** and the rate of formation of **4** from **2** were found (qualitatively) to depend on the concentration of the pyridine reagent. At the same pyridine concentration, the formation of **4** occurs much faster than that of **5**, so **4** can be easily prepared and isolated before a detectable amount of **5** is produced. Unlike **4a,b**, complex **4c** does not react further with 2-ethylpyridine (neat, 110 °C, 24 h) with or without cyclooctene present in the mixture.

Compounds **5a,b** each exist as two isomeric forms (NMR evidence). One isomer appears to be C<sub>2v</sub>-symmetric by NMR, while the other has C<sub>s</sub>-symmetry (Scheme 3, where the two phosphine arms above and below the NRe(N)<sub>2</sub> plane are omitted for clarity). We undertook a VT NMR study of **5b** and found that for either of the isomers, the <sup>1</sup>H NMR is essentially unchanged in the –60 to 80 °C range. Below –60 °C, the peaks due to the PNP ligand begin to broaden significantly but the peaks corresponding to the pyridine ring remain sharp. We have encountered such broadening of the PNP ligand resonances at temperatures below –60 °C in several Re and Ru complexes, and we attribute it to the slowed flexing of the PNP back-

bone.<sup>1,2,37,38</sup> The two isomers in **5a,b** are in equilibrium at 22 °C. No coalescence is observed for either of **5a,b** at 22 °C, and the same isomer ratio is observed for **5a** upon dissolution regardless of the sample handling history. Heating a solution of **5b** to 110 °C for 5 min and then rapidly cooling it to 22 °C produces a mixture of isomers with a 2:1 ratio in favor of the symmetric one. However, over 4 h at 22 °C, the ratio changes to ca. 5:1, and this ratio change is reversible. A single resonance corresponding to Re–C<sub>α</sub> in each of the C<sub>2v</sub>-symmetric isomers of **5a,b** is found at ca. 180 ppm in the <sup>13</sup>C NMR spectra, and a pair of corresponding resonances is found for each of the C<sub>s</sub>-symmetric isomers of **5a,b** at ca. 175 and ca. 204 ppm. The solution NMR studies are consistent with the interconversion between the isomers being slow on the NMR time scale even at ambient temperature and the observed spectra being those of individual isomers and are not time-averaged spectra of an isomeric equilibrium.

There are two possible C<sub>2v</sub> symmetric isomers (**5a(b)-I** and **5a(b)-III**). Solely on the basis of solution one-dimensional NMR evidence, it was not possible to determine which one is the experimentally observed C<sub>2v</sub> isomer. The crystallographic study of a single crystal (vide infra) obtained from the solution of **5a** determined the structure of the isomer in the crystal to be **5a-I**. DFT studies (vide infra) confirm the thermodynamic preference for the isomer **5-I**.

The transformation of **4** into **5** is a multistep process. During the reaction, intermediates **6a,b** (Scheme 4) are observed, but they are eventually fully converted into **5a,b**, respectively.

Compound **6a** was independently generated by exposure of **4a** to an atmosphere of H<sub>2</sub>. Quantitative formation of **6a** was not possible because **6a** itself competitively reacts with H<sub>2</sub> to produce **3a** and **1**. The NMR spectra of **6a** are those of a C<sub>s</sub>-symmetric species with a hydride signal (intensity 3H) observed at –5.44 ppm in <sup>1</sup>H NMR, a single <sup>31</sup>P NMR resonance observed at 48.7 ppm, and a triplet Re–C<sub>α</sub> resonance at 184.9 ppm in <sup>13</sup>C NMR. Similar <sup>31</sup>P and <sup>1</sup>H features were also observed for **6b,c**. The <sup>31</sup>P NMR resonances of **6a–c** can be selectively decoupled from only the alkyl hydrogens, resulting in a quartet from coupling to three hydrides.

Remarkably, **5a** undergoes no reaction with 1 atm of H<sub>2</sub> even at 90 °C. Since **5a** resists hydrogenolysis, it was intriguing to find out whether **5a** can be formed from 4-methylpyridine and **1** directly in an acceptorless dehydrogenation. Indeed, thermolysis of **1** in 4-methylpyridine at 120 °C (under static vacuum in a closed J. Young tube, i.e., gaseous products were *not* being removed) after 2 days produced a considerable amount of **5a** (60%) along with some unidentified products.

**Reactions of Bis-ortho-Substituted Pyridines.** Each of the pyridines **3a–c** possesses at least one aromatic C–H in the ortho position. Investigation of the thermolyses (110 °C) of **2** in the presence of bis-ortho-substituted pyridines **3d,e** revealed that ultimately the carbynes **7a,b** are formed instead of aromatic C–H activation products (Scheme 5).

While the aromatic C–H bonds are sterically shielded in **3e**, **3d** possesses at least one aromatic C–H bond sterically open to attack. The carbynes **7a,b** are characterized by the carbyne <sup>13</sup>C NMR resonance at ca. 270 ppm and a single hydride <sup>1</sup>H

(37) Watson, L. A.; Ozerov, O. V.; Pink, M.; Huffman, J. C.; Caulton, K. G. *J. Am. Chem. Soc.* **2003**, *125*, 8426.

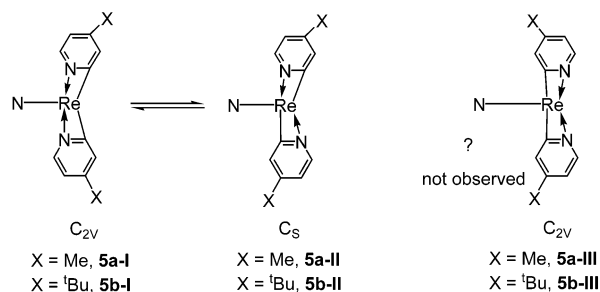
(38) Watson, L. A.; Coalter, J. N.; Ozerov, O. V.; Pink, M.; Huffman, J. C.; Caulton, K. G. *New J. Chem.* **2003**, *27*, 263.

Table 1. Summary of Crystal Data<sup>a</sup>

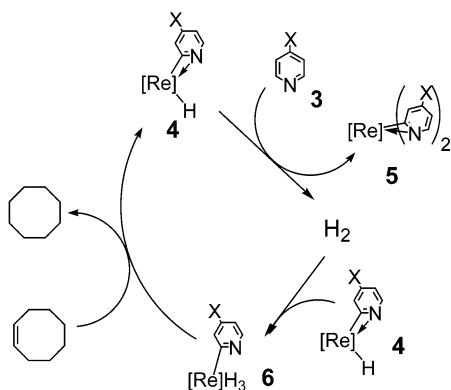
	4a	5a	8
empirical formula	C <sub>24</sub> H <sub>51</sub> N <sub>2</sub> P <sub>2</sub> ReSi <sub>2</sub>	C <sub>30</sub> H <sub>56</sub> N <sub>3</sub> P <sub>2</sub> ReSi <sub>2</sub>	C <sub>25</sub> H <sub>51</sub> N <sub>2</sub> P <sub>2</sub> ReSi <sub>2</sub>
formula weight	671.99	763.10	684.00
crystal color, size	black, 0.28 × 0.25 × 0.18 mm <sup>3</sup>	red, 0.20 × 0.20 × 0.08 mm <sup>3</sup>	black, 0.22 × 0.18 × 0.10 mm <sup>3</sup>
crystal system, space group	orthorhombic, <i>Pnma</i>	monoclinic, <i>P2/c</i>	monoclinic, <i>P2<sub>1</sub>/n</i>
<i>a</i> , Å	12.8870(4)	19.3458(8)	10.5307(4)
<i>b</i> , Å	16.9003(5)	10.7479(4)	14.7683(5)
<i>c</i> , Å	14.1618(4)	18.3294(7)	19.5511(7)
$\beta$ , deg		113.714(1)	92.604(1)
<i>V</i> , Å <sup>3</sup>	3084.36(16)	3489.4(2)	3037.46(19)
<i>Z</i>	4	4	4
$\rho_{\text{calcd}}$ , g/cm <sup>3</sup>	1.447	1.453	1.496
absorption coefficient, mm <sup>-1</sup>	4.135	3.666	4.201
absorption correction		semiempirical from equivalents	
max and min transmission	0.5231 and 0.3906	0.7580 and 0.5276	0.6787 and 0.4584
data/restraints/parameters	5763/57/238	9885/19/452	8869/0/305
goodness-of-fit on <i>F</i> <sup>2</sup>	1.106	1.025	1.064
final <i>R</i> indices [ <i>I</i> > 2 $\sigma$ ( <i>I</i> )]	<i>R</i> <sub>1</sub> = 0.0146, <i>wR</i> <sub>2</sub> = 0.0379	<i>R</i> <sub>1</sub> = 0.0266, <i>wR</i> <sub>2</sub> = 0.0588	<i>R</i> <sub>1</sub> = 0.0161, <i>wR</i> <sub>2</sub> = 0.0408
<i>R</i> indices (all data)	<i>R</i> <sub>1</sub> = 0.0160, <i>wR</i> <sub>2</sub> = 0.0386	<i>R</i> <sub>1</sub> = 0.0360, <i>wR</i> <sub>2</sub> = 0.0622	<i>R</i> <sub>1</sub> = 0.0181, <i>wR</i> <sub>2</sub> = 0.0419
largest difference peak and hole, e/Å <sup>3</sup>	1.170 and -0.900	1.526 and -0.705	1.757 and -0.387

<sup>a</sup> Goodness-of-fit =  $[\sum[w(F_o^2 - F_c^2)^2]/N_{\text{observns}} - N_{\text{params}})]^{1/2}$ , all data.  $R_1 = \sum(|F_o| - |F_c|)/\sum |F_o|$ .  $wR_2 = [\sum[w(F_o^2 - F_c^2)^2]/\sum [w(F_o^2)^2]]^{1/2}$ .

Scheme 3



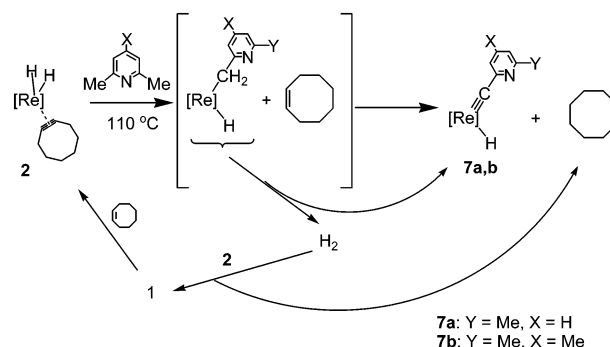
Scheme 4



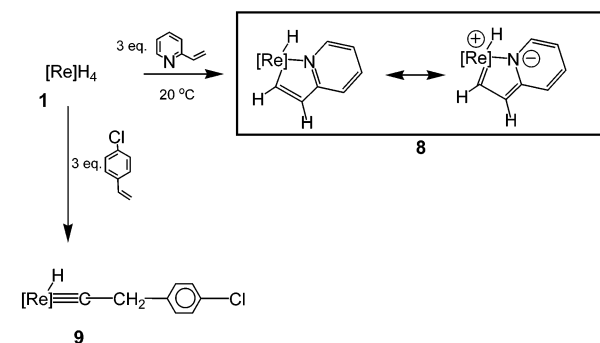
NMR resonance at ca. -9.2 ppm. The NMR spectra of **7a,b** very closely correspond to the spectra of related hydridocarbonyls with aliphatic substituents on the carbyne carbon.<sup>2,39</sup> At the intermediate stages, a small amount of complex **1** is observed, which completely disappears by the endpoint of the reaction. Thus, the initial benzylic oxidative addition produces cyclooctene and H<sub>2</sub>, and the hydrogenation of cyclooctene proceeds via the observable **1**.

**Reactions with 2-Vinylpyridine.** The reaction of (PNP)ReH<sub>4</sub> (**1**) with  $\geq 3$  equiv of 2-vinylpyridine (**3f**) at ambient temperature produces yellow-brown (PNP)ReH(pyridylvinyl) (**8**) in a quantitative (NMR) yield (Scheme 6) along with **3c**. If less than 3 equiv of 2-vinylpyridine is used in the reaction, then a mixture of **1**, **4c**, **6c**, and **8** is formed. Such a mixture is fully converted to **8** if additional (up to 3 equiv total) 2-vinylpyridine is added.

Scheme 5



Scheme 6



The C<sub>s</sub>-symmetric compound **8** displays a single Re-H resonance at ca. -5 ppm (td, *J*<sub>HP</sub>, *J*<sub>HH</sub>, 1H), six downfield <sup>1</sup>H NMR resonances, and the PNP signals. The downfield signals were analyzed by selective <sup>1</sup>H-<sup>1</sup>H decoupling experiments. There are four aromatic signals (d, t, t, d) and two vinylic ones (dd, d). The most downfield resonance (11.34 ppm, dd) shows coupling to both Re-H and the other vinylic hydrogen. In the <sup>13</sup>C NMR, a downfield resonance at ca. 234 ppm (triplet, *J*<sub>CP</sub>) is observed along with an appropriate number of other signals for nonmetal-bound sp<sup>2</sup>-carbons and the PNP system. The overall picture is consistent with the (PNP)ReH(pyridylvinyl) formulation (**8**) where vinyl is transoid to H and where there is

(39) McNeil, W. S.; DuMez, D. D.; Matano, Y.; Lovell, S.; Mayer, J. M. *Organometallics* **1999**, *18*, 3715.

a significant contribution of a carbene resonance form at the Re–C carbon. This was confirmed by single-crystal X-ray diffraction (vide infra).

**DFT Analysis of Pyridyl Re Compounds.** DFT<sup>40,41</sup> is a vital supplement to experimental studies not only because it allows the strengthening of conclusions derived from experiment but also because it can be a unique source of information with respect to energetics of reactions and energies and geometries of compounds not observed experimentally.

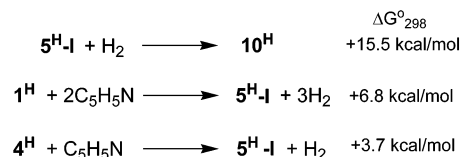
We used a model (H<sub>2</sub>PCH<sub>2</sub>SiH<sub>2</sub>)<sub>2</sub>N ligand (PNP<sup>H</sup>) and unsubstituted pyridyls in our DFT studies. Such model compounds will be denoted by superscript “H”. The calculations show that all species calculated adopt d<sup>4</sup> Re(III) ground states. The DFT-calculated structure of **4<sup>H</sup>** (Figure 1, from a starting geometry *without* a Re/N<sub>(py)</sub> bond) closely reproduces the important features of the X-ray structure of **4a**: the Si<sub>2</sub>N–Re distance is short, indicative of  $\pi$ -bonding contribution, and the pyridyl fragment is bound to Re in an  $\eta^2$ -fashion.

The DFT-optimized structure of **6<sup>H</sup>** (Figure 1) contains a classical hydride ligand as well as a dihydrogen ligand (d(H–H) = 0.940 Å), the latter being trans to the amido group of PNP. The Re–H distances to the hydrogens of the  $\eta^2$ -H<sub>2</sub> ligand are ca. 0.09 Å longer than the distance to the classical hydride ligand. The N of the pyridyl ligand is not coordinated to Re. This leaves only the  $\pi$ -lone pair of the amido ligand to complete the 18e configuration at Re, and indeed, the Re–N(Si)<sub>2</sub> distance is short (2.040 Å), indicative of a multiple-bond character.

DFT computational results were used to reinforce the conclusions about the nature of the isomers of **5a,b**. Experimentally, we observed only two isomers for each of **5a,b**. However, we set out to examine all three possible rotamers arising from rotation of the pyridyl group. The DFT-optimized geometries and corresponding energies of the model compounds (**5<sup>H</sup>-I–III**) are depicted in Figure 1. The most stable isomer is **5<sup>H</sup>-I**, the C<sub>2v</sub> symmetric rotamer. On the basis of this DFT finding (this was also the structure established crystallographically), we suggest that this is the predominant isomer of **5** observed in solution. The DFT-calculated energies correspond to the experimental observations extremely well. Thus, the difference ( $\Delta\Delta G_{298}$ ) between **5<sup>H</sup>-I** and **5<sup>H</sup>-II**, the next highest isomer in energy, is only 0.3 kcal/mol, in line with the observation of the 4:1 I/II ratio at rt in solution for **5a** (5:1 for **5b**). The third rotamer **5<sup>H</sup>-III** is calculated to be 2.9 kcal/mol higher in energy than **5<sup>H</sup>-I**. The fact that **5a(b)-III** was not detected in our NMR solution study allows us to estimate the possibility that it must be >2.7 kcal/mol higher in energy than **5a(b)-I**. However, in all three isomers, the pyridyl rings are approximately perpendicular to the PNPre plane, and one might expect that the neglect of steric bulk of the PNP ligand in the calculations will affect all three isomers equally. Omitting the para substituent on the pyridyl rings in calculations is not expected to have a significant effect on the results either, taking into account that for both Me and <sup>t</sup>Bu substituents observed, the K<sub>eq</sub> between **5a(b)-I** and **5a(b)-II** are very similar.

It is possible that the isomer **5<sup>H</sup>-III** is disfavored because the two ligands with the strongest trans influence (C of pyridyl)

### Scheme 7



are the closest to being trans to each other; however, the preference for a particular orientation of the pyridyl ring is rather small. In all rotamers of **5**, there exists a competition between the  $\pi$ -lone pair of the amido and the lone pair on N of pyridyl for the empty coordination site at Re. Thus, in **5<sup>H</sup>-I**, both pyridyl rings are  $\eta^2$ -coordinated and the metal center does not need  $\pi$ -donation from the amido to obtain an 18e configuration. Accordingly, the Re–N(Si)<sub>2</sub> distance is long at 2.153 Å, while the N–Si distances are short at 1.723 Å. In **5<sup>H</sup>-III**, and in contrast to the drawing in Scheme 3, only one of the pyridyl rings is  $\eta^2$  (N<sub>py</sub>–Re distances of 2.165 and 3.064 Å), and **5<sup>H</sup>-III** features a short Re–N(Si)<sub>2</sub> distance (2.033 Å) and long N–Si distances (av 1.763 Å), consistent with the proposed N→Re  $\pi$ -donation.

In **5<sup>H</sup>-II**, one of the pyridyl rings is unambiguously  $\eta^2$  (d(Re–N<sub>py</sub>) = 2.149 Å), while the other displays an “elongated”  $\eta^2$  coordination (d(Re–N<sub>py</sub>) = 2.336 Å). At the same time, the values of the Re–N(Si)<sub>2</sub> distance (2.090 Å) and the N–Si distances (av 1.735 Å) are between those of **5<sup>H</sup>-I** and **5<sup>H</sup>-III**. The bonding picture in **5<sup>H</sup>-II** may be described as partial  $\pi$ -donation from the amido being complemented by partial  $\sigma$ -donation from the second N<sub>py</sub>.

The DFT computations also help assess the energetics of the reactivity of **5** (Scheme 7). The  $\Delta G_{298}^{\circ}$  for addition of H<sub>2</sub> to **5<sup>H</sup>-I** to give **10<sup>H</sup>** (Figure 1) was calculated to be 15.5 kcal/mol, consistent with the experimental observation of inertness of **5** toward H<sub>2</sub> as being thermodynamic in origin. On the other hand, for the reaction of **1<sup>H</sup>** with pyridine to produce **5<sup>H</sup>**,  $\Delta G_{298}^{\circ}$  was calculated to be only 6.8 kcal/mol. This value is not inconsistent with the experimental observation of the forward reaction, given that the pyridine reagent is used in large excess. The reaction of **4<sup>H</sup>** with pyridine to give **5<sup>H</sup>** and H<sub>2</sub> is calculated to have  $\Delta G_{298}^{\circ}$  of 3.7 kcal/mol. This is in accord with the experimental observation of this reaction because at least some of the produced H<sub>2</sub> is removed by either hydrogenation of cyclooctene or by complexation to **4**.

**X-ray Structure Determinations.** In the structure of **4a** (Figure 2, grown by cooling a solution in *neo*-hexane to –30 °C), a disorder of the PNP backbone is present that results in the presence of a crystallographic mirror plane in the molecule. The pyridyl moiety is  $\eta^2$  and the hydride atom position was located unambiguously. The overall geometry about the Re center can be described as distorted octahedral with H(1r) and C(10) deviating from idealized octahedral positions by bending away from the amido N(1). The bending of C(10) and H(1r) away from N(1) approximately in the plane of the N(1) lone pair is reminiscent<sup>2</sup> of the similar bending of the two hydrides away from the N(amido) in the structure of (PNP<sup>Cy</sup>)ReH<sub>4</sub>. Such a distortion rehybridizes the orbitals to enhance the multiple bonding between Re and N(1) and to strengthen the  $\sigma$ -bonds to C(10) and H(1r). Indeed, the Re–N(1) distance is short at 2.01 Å, indicative of significant  $\pi$ -bonding between Re and N(1). The Re–N(2) bond is considerably longer at 2.17 Å, and the N(1)–Re–N(2) angle is 168°.

(40) Koch, W.; Holthausen, M. C. *A Chemist's Guide to Density Functional Theory*, 2nd ed.; Wiley-VCH: Weinheim, Germany, 2001.

(41) Frenkel, F. *Introduction to Computational Chemistry*; John Wiley & Sons: Chichester, England, 1999.

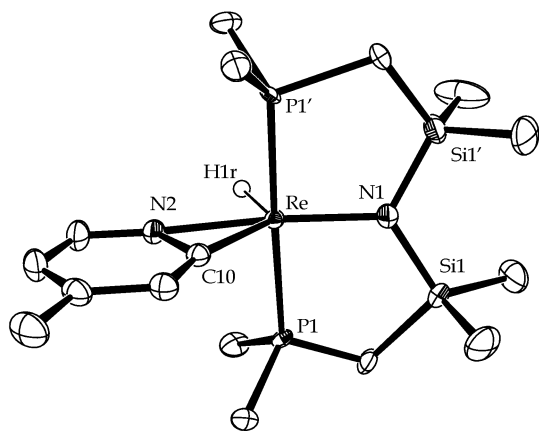


**Figure 2.** ORTEP plot of **4a** (Me groups of *i*-propyls and all Hs except Re–H are omitted for clarity; disorder not shown). Selected bond distances (Å) and angles (°): Re–N(1), 2.0136(16); Re–C(10), 2.028(2); Re–N(2), 2.1653(16); Re–H(1r), 1.65(4); N(1)–Si (average), 1.7493(12); N(1)–Re(1)–N(2), 168.47(7); N(1)–Re(1)–C(10), 131.35(7); N(1)–Re(1)–H(1r), 109.5(13).

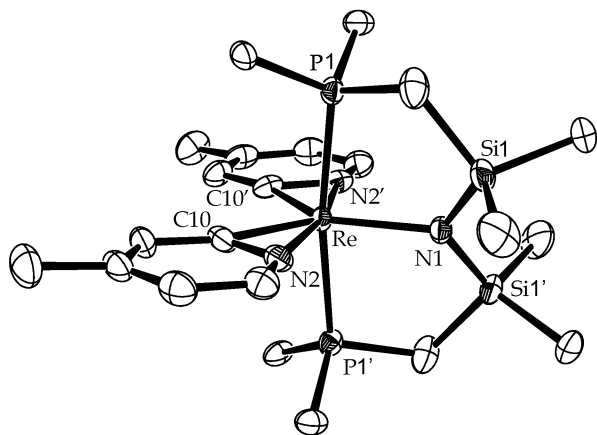


**Figure 3.** ORTEP plot of one of the independent molecules of **5a** (Me groups of *i*-propyls and all Hs are omitted for clarity). Selected bond distances (Å) and angles (°) in the two independent molecules: Re–N(1), 2.147(3), 2.155(3); Re–C(10), 2.020(3), 2.018(3); Re–N(2), 2.133(3), 2.138(2); Re–P, 2.3908(7), 2.3855(7); N(1)–Si(1), 1.7083(15), 1.7087(16); P–Re–P', 171.37(3), 171.43(3); N(1)–Re–N(2), 95.80(6), 96.13(6); N(1)–Re–C(10), 133.70(8), 133.97(8); C(10)–Re–C(10'), 92.59(17), 92.06(16).

A crystal of the  $C_{2v}$ -symmetric isomer (Figure 3) was obtained from the mixture of isomers of **5a**. The presence of a *para*-methyl substituent, together with the refinement of the X-ray data, leaves no ambiguity in C vs N determination. The unit cell contains four molecules, two halves of which are in the asymmetric unit. Thus, the asymmetric unit consists of two halves of two independent half-molecules. The differences in the geometric parameters between the two half-independent molecules are not chemically significant. The geometry about the Re center can be described as approximately pentagonal bipyramidal with P atoms occupying the apical positions. The N(2) atoms of the  $\eta^2$ -pyridyl ligands are cisoid to the amido N(1). The Re–C(10) distances (2.019 Å) and the Re–N(2) (2.136 Å) distances in **5a** are comparable to those in **4a**. The Re–N(1) distance of 2.15 Å is much longer than the corresponding distance in **4a**, consistent with a decrease to single-bond character in **5a**. Thus, coordination of the pyridine N is preferred over the N(1)→Re  $\pi$ -donation. However, the observed

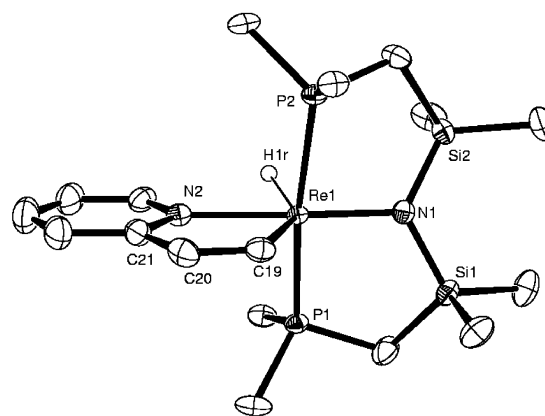


**Figure 4.** ORTEP plot of **8** (Me groups of *i*-propyls and all Hs except Re–H are omitted for clarity). Selected bond distances (Å) and angles (°): Re(1)–P(1), 2.3923(4); Re(1)–P(2), 2.3757(4); Re(1)–H(1r), 1.69(2); Re(1)–N(1), 2.0307(14); Re(1)–N(2), 2.2081(15); Re(1)–C(19), 2.0156(18); N(1)–Si(1), 1.7425(15); N(1)–Si(2), 1.7443(15); P(1)–Re(1)–P(2), 170.828(15); N(1)–Re(1)–N(2), 168.87(6); H(1r)–Re(1)–C(19), 140.0(9); C(19)–Re–N(1), 119.63(7); N(1)–ReH(1r), 99.2(9).

exchange between rotameric forms of **5a,b** must proceed via an  $\eta^1$ -pyridyl structure, and it is highly probable that the unsaturation created by the dissociation of a pyridyl N is relieved by the  $\pi$ -donation from the amido ligand, lowering the activation barrier for this isomerization.

The structure of **8** (Figure 4) is conceptually similar to that of **4a**. The plane of the pyridylvinyl ligand and the hydride is approximately perpendicular to the PNP plane, and C and H are similarly bent away from the amido N. The Re–N(1) bond is short at 2.0307(14) Å, indicative of multiple bonding between Re and N(1). The Re–N(2) distance (2.2081(15) Å) is somewhat longer than the corresponding distances in **4a** and **5a**, but the Re–C distance (2.0156(18) Å) is slightly shorter than Re–C distances in **4a** and **5a**. The elongation of the Re–N(2) bond is probably a consequence of being a part of a larger metallacycle.

The Re–C distances in **4a**, **5a**, and **8** are shorter than might be expected for a single  $C(sp^2)$ –Re bond. For example, several (hydridotrispyrazolylborato)Re complexes with Re–Ph bonds were structurally characterized and the ca. 2.10–2.14 Å Re–Ph distances were reported.<sup>39,42</sup> A Re– $C(sp^2)$  bond distance of ca. 2.12 Å was reported<sup>43</sup> in a vinyl–Re complex resulting from the insertion of acetylene dicarboxylate into a Re–H bond. It may also be noted that the Re–C distances in **4a**, **5a**, and **8** are comparable to the multiple Re–N(amido) bond in **4a** and **8**. For **4a** and **5a**, this may be primarily a consequence of a tight three-membered metallacyclic subunit. For **8**, the shortened Re–C distance is in accord with the contribution of the carbene resonance structure (vide supra, Scheme 6), which effectively reflects  $\pi$ -donation from Re into the pyridylvinyl  $\pi$ -system. The contribution of this resonance structure affects other bond lengths in the five-membered metallacycle in **8** and appears to be somewhat greater than in the related Ru compound **11**<sup>44</sup> (Scheme 8). It is remarkable that a  $d^4$  Re center in **8** behaves as a more potent  $\pi$ -base than a  $d^6$  Ru center in **11**. This might be attributed to the amide nitrogen in PNP.

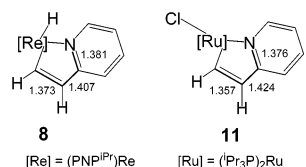
(42) Matano, Y.; Northcutt, T. O.; Brugman, J.; Bennett, B. K.; Lovell, S.; Mayer, J. M. *Organometallics* **2000**, *19*, 2781.

(43) Kim, Y.; Gallucci, J.; Wojcicki, A. *Organometallics* **1992**, *11*, 1963.

(44) Coalter, J. N.; Streib, W. E.; Caulton, K. G. *Inorg. Chem.* **2000**, *39*, 3749.



## Scheme 8



## Discussion

Complex **2** can be considered as the product of oxidative addition of two vinylic C–H bonds of cyclooctene onto the “naked” (PNP<sup>iPr</sup>)Re fragment. In other words, it is the latter fragment combined with the elements of cyclooctene. Thus, **2** can serve as a surrogate for the inaccessible (PNP<sup>iPr</sup>)Re by having cyclooctene be replaced on the monovalent Re center by (elements of) another organic molecule. Furthermore, cyclooctene is not always an innocent byproduct but can act as a hydrogen acceptor. We were interested in whether **2** can serve as a synthetic equivalent of (PNP<sup>iPr</sup>)Re in reactions with alkyl-substituted pyridines and in the selectivity of benzylic vs aromatic C–H activation. Our findings indicate that the activation of the ortho C–H bond in a pyridine ring is the preferred mode of reactivity and that the products of benzylic activation are only observed for substrates with substituents in both ortho positions.

If both ortho positions bear methyl substituents, then carbynes resulting from the activation of such methyl groups are exclusively produced. The obvious preference for the formation of the ortho CH activation product, through either aromatic or aliphatic activation, must stem from the influence of the pyridine nitrogen. It is likely that this nitrogen exerts both kinetic and thermodynamic influences on the regioselectivity of the reported reactions. The aryl activation products contain  $\eta^2$ -bound pyridyl ligands. Additional binding of N is a feature unattainable for purely hydrocarbon aromatics, and it must add to the thermodynamic stability of the ortho aromatic activation products of pyridines. Neither can such stabilization be achieved in the case of meta or para activation of pyridines. Therefore, when meta and para aromatic C–H bonds are the only ones available, aliphatic activation to produce carbynes occurs instead.

We believe that the initial coordination of pyridines via an N→Re dative bond dramatically decreases the activation barrier of these reactions by bringing the C–H bonds into the vicinity of the metal center. A similar effect was ascribed to the heteroatom coordination in C–H activation of ethers and amines by Os and Ru complexes.<sup>45,46</sup> That the aromatic activation of the ortho CH bonds of pyridines is *thermodynamically* and not just *kinetically* preferred is evident from the intermediacy of **3c**, **4c**, and **6c** in the reaction of **3f** with **1** (vide supra). Because

the reaction proceeds by hydrogenation of the double bond of **3f**, it implies that the metal is at some point bound to the carbons of the hydrogenated ortho substituent yet produces aromatic activation products and not the possible carbyne. Notably (Scheme 6), 4-chlorostyrene produces exclusively the 4-chlorobenzylcarbyne complex **9**. Compound **8** may be viewed as a vinyllogue of compounds **4**: its apparently greater stability may be ascribed to some relief of strain on going from a three-membered metallacycle to a five-membered one. One obvious alternative to the formation of C–H activation products is the formation of simple  $\eta^1$ -pyridine complexes of (PNP<sup>iPr</sup>)Re<sup>I</sup>. Such a coordination mode, however, would not serve to relieve the highly electron-rich Re center of electron density. Our studies have shown that reconstruction of organic fragments on (PNP<sup>R</sup>)Re follows precisely that pattern: the metal reacts to attain higher formal oxidation states via oxidative addition processes and/or isomerization of organic fragments into stronger  $\pi$ -acids (e.g., alkenes to metal-bound carbenes or hydrido carbynes).<sup>1,2</sup>

The observation of **6a,b** in reactions of **2** with **3a,b** deserves special mention. Complexes **4a,b** are the initial products of this reaction. We propose that some H<sub>2</sub> is liberated into the reaction mixture and then trapped by **4** to form **6** (Scheme 4). Cyclooctene serves to dehydrogenate **6** back to **5**, but this dehydrogenation is slow enough for **6** to be observed. We believe that the required free H<sub>2</sub> is generated upon oxidative addition of **3a,b** to **4** and that the putative H<sub>2</sub> complex of **5** is unstable with respect to H<sub>2</sub> loss. This is supported by DFT calculations on the model compound and by the experimental observation that **5a** does not bind H<sub>2</sub> at 22 °C or react with H<sub>2</sub> under more forcing conditions (1 atm H<sub>2</sub>, 90 °C, 1 h).

The failure of **4c** to react further with **3c** can be rationalized on steric grounds. Unlike **4a,b**, **4c** carries an *ortho*-ethyl substituent, which, taking into account the  $\eta^2$ -coordination mode of the ethylpyridyl ligand, provides steric shielding of the metal center. This is compounded by the fact that **3c** also carries an *ortho*-ethyl substituent, which increases the steric obstacles for the precoordination of **3c** to **4c**. Besides such kinetic reasoning, it may be thermodynamically unfavorable to form **5** with both  $\eta^2$ -pyridyl units bearing an ortho substituent due to steric repulsion in the product.

**Acknowledgment.** This work was supported by the Department of Energy. L.A.W. expresses thanks to NSF for a Graduate Fellowship.

**Supporting Information Available:** Full results from DFT-calculated structures and full crystallographic information files (CIF). This material is available free of charge via the Internet at <http://pubs.acs.org>.

JA036999I

(45) Coalter, J. N.; Ferrando, G.; Caulton, K. G. *New J. Chem.* **2000**, *24*, 835.

(46) Ferrando-Miguel, G.; Coalter, J. N.; Gerard, H.; Huffman, J. C.; Eisenstein, O.; Caulton, K. G. *New J. Chem.* **2002**, *26*, 687.